Optimization and Test of 120mm LARP Nb_3Sn Quadrupole Coils Using Magnetic Mirror Structure

R. Bossert, G. Ambrosio, N. Andreev, M. Anerella, E. Barzi, S. Caspi, D. Cheng, G. Chlachidze, D. Dietderich, H. Felice, P. Ferracin, A. Ghosh, A.R. Hafalia, V.V. Kashikhin, M. Lamm, A. Nobrega, I. Novitski, G.L. Sabbi, J. Schmalzle, P. Wanderer, A.V. Zlobin

***Abstract*—The US-LARP collaboration is developing a new generation of large-aperture high-field quadrupoles based on Nb_3Sn superconductor for the LHC upgrades. The development and implementation of this new technology involves the fabrication and testing of series of model magnets, coils and other components with various design and processing features. New 120-mm HQ coils made of Rutherford cable, one with an interlayer resistive core, and both with optimized reaction processes, were fabricated and tested using a quadrupole mirror structure under operating conditions similar to those in a real magnet. The coils were instrumented with voltage taps and strain gauges to study the mechanical and quench performance. Quench antenna and temperature gauges were installed in the mirror structure to measure the coil temperature and locate quench origins. This paper presents details of the coil design and fabrication procedures, coil assembly and pre-stress in the quadrupole mirror structure, and coil test results.**

***Index Terms*—LARP, quadrupole coil, magnetic mirror, magnet test.**

I. INTRODUCTION

A NEW generation of accelerator magnets is being developed based on Nb_3Sn superconductor. One application of this research, currently being pursued by the US-LHC Accelerator Research Program (LARP) [1], is to develop an interaction region (IR) quadrupole for an eventual upgrade to the LHC.

An efficient way to optimize coils is to test them in a magnetic mirror structure. This allows individual coils to be tested under conditions similar to those of an actual magnet. Only one coil needs to be made instead of four, minimizing cost and turnaround time. Several short (1 m long) and one long (4 m long) coil have been successfully tested using quadrupole mirrors [2-5]. This paper describes the construction and testing of HQM01 and HQM02, quadrupole mirrors using coils with 120 mm bore and wide 15 mm cable, similar to the aperture size needed for the eventual LHC IR region upgrade.

Manuscript received 12 September 2011. This work supported by the Fermilab Research Alliance, LLC, under contract No. DE-AC02-07CH11259 with the U.S. Department of Energy: by the Director, Office of Science, High Energy Physics, U.S. Department of Energy under contract No. DE-AC02-05CH11231, and partially by the DOE through the US-LHC Accelerator Research Program (LARP).

R. Bossert, G. Ambrosio, N. Andreev, E. Barzi, G. Chlachidze, V.V. Kashikhin, M. Lamm, A. Nobrega, I. Novitski, and A.V. Zlobin are with Fermi National Accelerator Laboratory, P.O. Box 500, Batavia, Il. USA (phone: 630-840-2867, fax: 630-840-8079, e-mail: bossert@ fnal.gov).

S. Caspi, D. Cheng, D. Dietderich, H. Felice, P. Ferracin, A.R. Hafalia and G.L. Sabbi are with Lawrence Berkeley National Laboratory, Berkeley, CA 94720 USA.

M. Anerella, A. Ghosh, J. Schmalzle and P. Wanderer are with Brookhaven National Laboratory, Upton, NY, 11973-5000 USA.

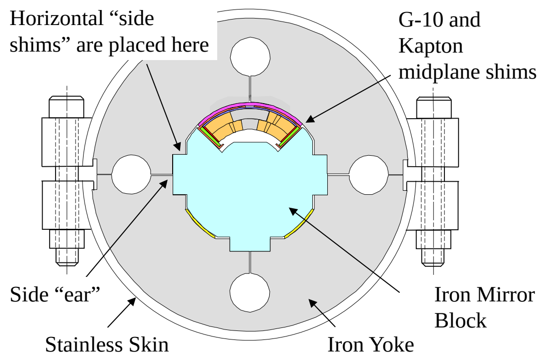

Fig. 1. HQ mirror structure.

II. HQ MIRROR STRUCTURE AND CONSTRUCTION

The HQ mirror assembly, including 120 mm quadrupole coil, yoke and skin is shown in Fig. 1. It is similar to the structure used for 90 mm TQ coils [2-4]. The magnetic flux distribution is similar to that of real quadrupoles [6], [7] and is shown in Fig. 2. Coil preload is provided by a 12 mm thick stainless steel skin and controlled by a series of shims placed radially and azimuthally on the coil, and to the upper surface of the side "ears" on the mirror block.

HQM01 and HQM02 contained coils HQ12 and HQ13 respectively. Table 1 describes the specific properties of the two optimized coils.

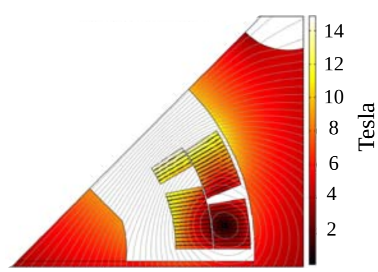

Fig. 2. HQ mirror cross section with magnetic flux distribution at 20 kA. Peak field at inner pole is 14.9 T.

TABLE 1 COIL SPECIFIC FEATURES

Coil #	Cable	Cable Ins.	Az. Space for Expansion (L 1/L 2)	Axial gap for Contraction (mm/m)
HQ12	SS core	S2 glass sleeve	5.4%/4.6%	1
HQ13	w/o core	S2 glass sleeve	7.6%/6.3%	2.75

The coils were made using 35 strand Rutherford cable with 0.80 mm diameter RRP strand of 54/61 sub-element design produced by Oxford Superconductor Technologies, Inc. The strand has a sub-element size of 70-80 µm, a copper fraction of 49.2% and a twist pitch of 12 mm, and a nominal J_c(4.5 K, 12 T) of 2900 A/mm^2. The cable in coil HQ12 included a 25 µm thick by 8mm wide stainless steel core. Both cables with and without stainless steel core were produced at Lawrence Berkeley National Laboratory (LBNL). Short sample currents for each coil are based on extracted strand measurements fit with the scaling law described in [8] including a self-field correction and assuming zero strain in the strand.

Coil end parts were made of 304 stainless steel to match coil azimuthal thermal contraction while poles were made from a titanium alloy to minimize thermal contraction in the axial direction. Both coils had the space for coil expansion during reaction increased to reduce the azimuthal pressure on the coil, HQ12 by directly increasing the azimuthal space in the reaction mold, and HQ13 by eliminating one mid-plane turn in each layer. For comparison, the azimuthal space allowed for cable expansion in previous HQ coils was only 2%. HQ magnets with these coils have been limited to ~ 85% of their short sample limit (SSL), possibly due to strand damage or degradation from excessive compaction during reaction [9]. HQ13 also had the axial gap between pole pieces increased to allow more room for axial contraction during reaction.

Both coils were instrumented with strain gauges on the inner surface of the coil pole. Coil inner surface gauges were configured in two full bridges, one each in the azimuthal and longitudinal direction. The structure included gauges on the exterior surface of the shell and on the end preload "bullets".

The coil is insulated from ground by Kapton® sheets. The thickness of Kapton is adjusted to achieve the desired preload at room temperature. Before magnet assembly, the cross section size is measured in its free state on a coordinate measuring machine. The measured size is used to determine the amount of mid-plane shim, based on previous experience and finite element analysis. Shims are also placed onto the horizontal surface of the side "ears" as shown in Fig. 1.

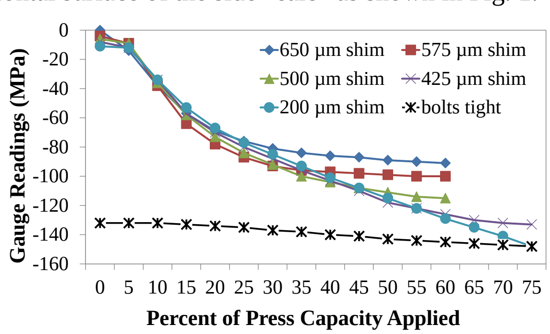

Fig. 3. HQM01 azimuthal preloads during pressing. Horizontal axis denotes % of press capacity, where full press capacity is 900,000 kG.

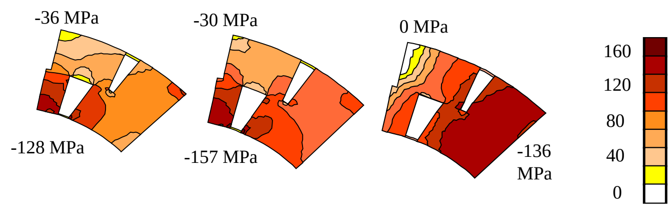

Fig. 4. Coil stress distributions in HQM structure at room temperature, 4.5K 0A and at 4.5K 17kA magnet current.

The side shims are used to adjust the preload during pressing and control the preload during cool-down.

The structure is placed into a hydraulic press and the pressure is increased until the desired preload is achieved (verified by the strain gauges). Then the press is released, a specified amount of shim is removed, and the pressure is reapplied until the strain gauges reach the same value as they had before the shims were removed. The bolts are then tightened, leaving an open area into which the structure can contract during cool-down, increasing the preload.

The coil preload was done using five separate pressings. After an initial pressing with a "side shim" of 650 µm, shims were removed between pressings in increments of 75 µm, until the final desired preload was achieved with a side shim of 425 µm. The "cool-down" gap of 225 µm was then added by reducing the amount of side shims to 200 µm. The final pressing was then completed and the bolts were tightened to close the structure. Strain gauge readings during this process are shown in Fig. 3 for HQM01. Azimuthal coil pre-stresses of HQM01 and HQM02 at room temperature were 132 and 130 MPa respectively, with the same space left for contraction during cool-down in both cases. Fig. 4 shows the expected stress distribution inside the structure at room temperature, 4.5 K and at 17 kA. As in all mirrors, a load of 10 kN was applied to each end through the 50 mm thick end plates.

III. TEST RESULTS

HQM01 and HQM02 were tested at Fermilab's Vertical Magnet Test Facility [10] in May and September 2011 respectively. Tests were performed in boiling liquid helium at 4.6 K and at lower temperatures for the temperature dependence study. Quench positions were determined by voltage taps and a quench antenna.

A. *Quench History*

At the start of HQM01 training at 4.6 K, large voltage spikes caused by flux jumps [11] triggered the quench protection system several times. In order to be higher than these spikes, the detection thresholds of the quench detection system were increased at low currents up to 2-3 volts. In addition it was necessary to increase the ramp rate at low currents in order to improve the stability of the conductor by eddy-current heating. The Voltage Spike Detection System (VSDS) [12] was used for recording the voltage across the two half-coils at a high sampling rate (100 kHz). The VSDS data was used for adjusting the quench detection thresholds. The largest amount of spikes were detected around 1000 A and maximum voltages varied from 0.1 to 0.55 V. Similar voltage thresholds were used for quench detection in HQM02.

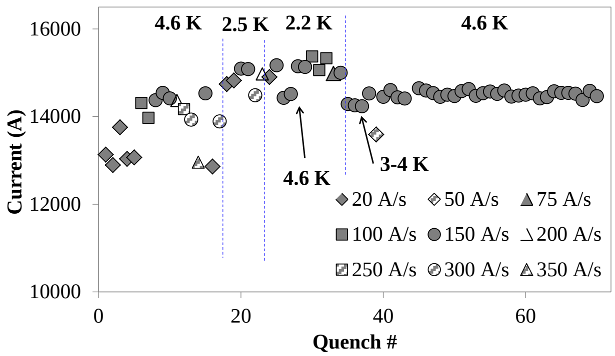

Fig. 5. HQM01 quench history with bath temperature and current ramp rate.

HQM01 quench history is presented in Fig. 5. The first two quenches at 20 A/s started in the mid-plane turn of the inner coil layer. The following quench developed in the pole turn of the inner coil layer, but then two quenches initiated again in the mid-plane segment, at approximately the same current 12.9-13.1 kA without signs of training.

When the ramp rate was increased to 100 A/s quench current reached 14-14.3 kA, but again, one quench developed in the pole turn followed by others in the mid-plane segment. Further increase of ramp rate showed that the quench current reached its maximum at a ramp rate of 150 A/s, then gradually decreased at higher ramp rates.

Finally quench current reproducibility was demonstrated at the 20 A/s and 150 A/s ramp rates - the coil quenched in the same mid-plane segment and at the same currents.

The test continued at lower temperatures of 2.2-2.5 K. Quench current increased at all ramp rates, but the mid-plane segment continued to limit the magnet performance.

At the end of the test several quenches were performed at 4.6 K for quench protection studies. Results of this study are reported in [13]. The residual resistivity ratio (RRR) of HQ12 coil was measured during magnet warm up, with values varying from 260 to 320.

In total, 70 quenches were performed on HQM01 (with coil HQ12), and in only 5 cases did a quench develop in the pole turn area. The magnet reached 14.6 kA or 82% of the short sample limit at 4.6 K and 15.4 kA (77%) at 2.2 K.

HQM02 (with coil HQ13) showed short training at both 4.6 K and 2.2 K temperatures (see Fig. 6). All training quenches were initiated in the pole-turn blocks, i.e. in the high field area. At 4.6 K, HQM02 reached a maximum quench current of 16.8 kA, which is 91% of its short sample limit (SSL) based on witness sample data. HQM02 showed good stability and an expected increase of quench current at 2.2 K. Quench plateau at 2.2 K was established at 18.2 kA (89% of SSL). The RRR of HQ13 coil segments varied from 220 to 285.

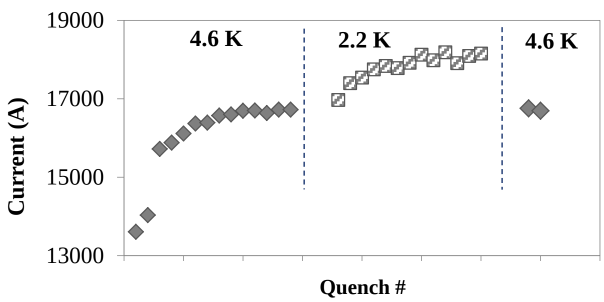

Fig. 6. HQM02 training quenches at 4.6 K and 2.2 K.

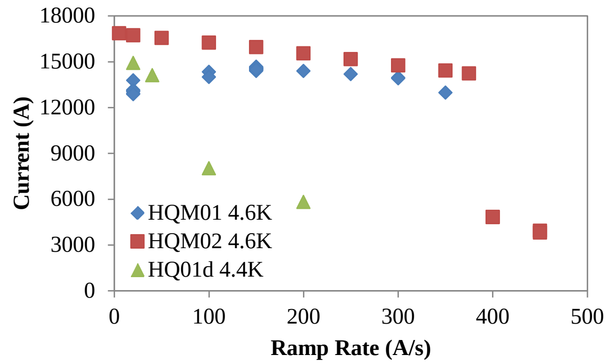

Fig. 7. HQM01 and HQM02 ramp rate dependence. HQ01d ramp rate dependence is also shown for comparison.

B. *Ramp Rate and Temperature Dependences*

Ramp rate dependence of the quench current of HQM01 and HQM02 at 4.6K is presented in Fig. 7. Ramp rate dependence of HQ01d (full magnet with similar RRP-54/61 strand, but without a stainless steel core in the cable) is also shown at 4.4K for comparison [14]. Since HQM01 demonstrated erratic quench performance at low ramp rates, all currents are shown for multiple quenches at the same ramp rate. Almost all quenches at all ramp rates occurred in the mid-plane area. The lower sensitivity to the current ramp rate observed for HQM01 is due to the higher inter-strand resistance in the cable controlled by the stainless steel core.

In HQM02, almost all quenches started in the pole-turn block, only quenches at ramp rates 400 A/s and higher were located in the mid-plane blocks of both the inner and outer layers. Quench current suddenly drops for ramp rates of 400 A/s at 4.6 K and for 450 A/s at 2.2 K.

Comparing ramp rate dependences of HQM02 and HQ01d both with cable without a core, one can notice that HQM02 demonstrates unexpectedly low ramp rate sensitivity. This is partially, but not fully, explained by a slight difference in the size of the field component perpendicular to the cable in the two structures. Another explanation could be the higher inter-strand resistivity in coil HQ13 due to unrestricted coil expansion during reaction as well as possible epoxy penetration inside the cable during impregnation.

Temperature dependence of the quench current is presented in Fig. 8. For HQM01, quenches at the peak performance of 150 A/s are shown. Ramps at intermediate temperatures (3 K and 4 K) were done during the warm-up from 2.2 K to 4.6 K. At 2.2-2.5 K quench currents are on average slightly higher and at intermediate temperatures slightly lower than at 4.6 K.

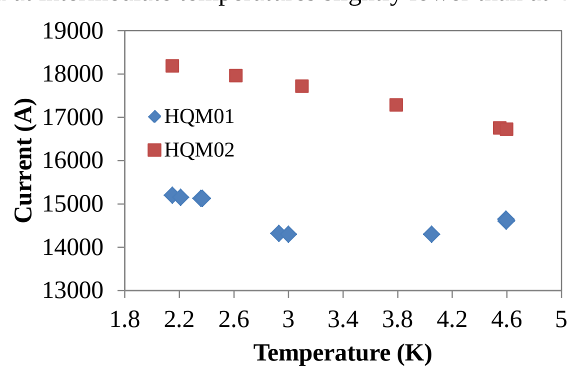

Fig. 8. Temperature dependence for HQM01 and HQM02.

For HQM02, the quench current dependence on magnet temperature was measured after magnet training at 2.2 K at a ramp rate of 20 A/s. HQM02 showed stable and reproducible quenches over the entire temperature range from 2.2 to 4.6 K.

The noticeable difference of temperature dependences for HQM01 and HQM02 could be also attributed to the differences of coil design and fabrication process.

C. Strain Gauges

Strain gauge data in HQM01 and HQM02 are almost identical for the magnet cool-down, training and warm-up. Strain gauges mounted azimuthally to the outside shell (skin) showed the expected strain increase during cool-down and were flat as expected during excitation. End load increased as expected during cool-down and during excitation. Azimuthal gauge readings [15] placed on the interior pole surface showed some inconsistencies during cool-down, possibly due to slight coil bending within the structure.

IV. Discussion of HQM01 and HQM02 Test Results

Most HQM01 quenches developed in a low field area – in the mid-plane turns. Erratic quenches in the mid-plane segment could be related to conductor damage resulting in reduced strand stability. The “reversed” ramp rate dependence observed at low ramp rates could then be explained by the larger heat generated during faster ramp rates. The heat decreases the critical current of the conductor and therefore increases its stability.

Both coils were tested in an identical structure, and under identical preload conditions. The same Nb_3Sn RRP 54/61 strand is used in both coils, but without a SS core in the conductor and with more room allowed for expansion during reaction of coil #13 in HQM02.

A series of HQ coils assembled in a shell-type mechanical structure (HQ01) had been previously tested at LBNL [9, 14]. Training performance of HQM01 and HQM02 at 4.6 K is compared with the HQ01a/d magnet performance at 4.4 K in Fig. 9.

HQ01d demonstrated better performance than HQ01a, reaching 86% of its expected short sample limit. The (only 3) training quenches of HQM01 at 4.6 K (developed in the pole turn block) are consistent with the HQ01d performance. Limitation in the inner-layer mid-plane segment did not allow further training of HQM01. Coil HQ13 in HQM02 showed the best training performance so far among all HQ coils.

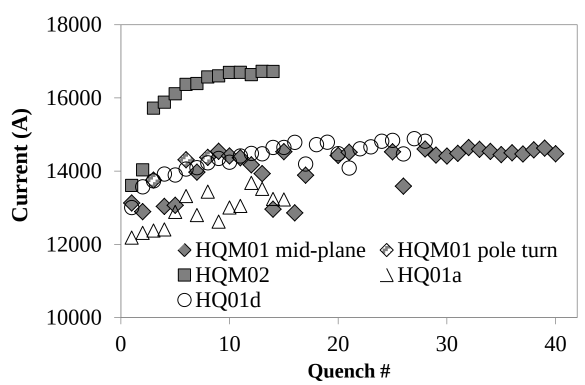

Fig. 9. Comparison of HQM01, HQM02 and HQ01a/d quenches at 4.4-4.6 K. Only first 40 quenches are shown for HQM01.

V. Conclusion

Two 120 mm bore LARP quadrupole coils (HQ12 and HQ13) of the HQ design have been tested in a quadrupole mirror structure under identical conditions. Both coils were made with additional space for azimuthal expansion than the baseline HQ coils. In addition coil HQ12 was made of cable with a core inside the cable. The goal of this experiment was to assess the effect of reduced coil compaction during reaction and the cable core on the coil quench performance.

Coil HQ13 reached 91% of its critical current limit, while coil HQ12 reached only 82% with almost all quenches in the low field area near the inner layer mid-plane. Insufficient space for azimuthal coil expansion and/or axial contraction during reaction as well as the core in the cable may have caused conductor damage during fabrication and increased instability in coil HQ12. As a result, future HQ coils will be fabricated with increased space for the coil during reaction.

Test results also confirmed the efficiency of the stainless steel core in suppressing eddy currents in the cable. The effect of the cable core on coil training needs further investigation.

Acknowledgment

The authors thank S. King, J. Swanson, D. Horler and C. Kozy for technical work during coil construction, J. Alvarez, S. Gould, S. Johnson, R. Jones, L. Ruiz and M. Whitson during assembly and W. Mumper and F. Lewis during testing.

References

[1] S.A. Gourlay et al., “Magnet R&D for the US LHC Accelerator Research Program (LARP)”, *IEEE Transactions on Applied Superconductivity*, Vol. 16, No 2, pp. 324-327, June 2006.

[2] A.V. Zlobin et al., “Testing of Nb_3Sn Quadrupole Coils Using Magnetic Mirror Structure,” *Advances in Cryogenic Engineering*, vol. 55B, pp. 1031-1038, 2010.

[3] N. Andreev et al., “Magnetic Mirror Structure for Testing Shell-type Quadrupole Coils”, *IEEE Trans. on Applied Supercond.*, vol. 20, no. 3, pp. 288-291, Jun. 2010.

[4] G. Chlachidze, et al., “The Study of Single Nb_3Sn Quadrupole Coils Using a Magnetic Mirror Structure”, *IEEE Transactions on Applied Supercond*., vol. 21, no. 3, pp. 1692-1695, June 2011.

[5] R. Bossert et al., “Fabrication and Test of 4 m long Nb_3Sn Quadrupole Coil Made of 114/127 RRP Strand”, presented at CEC2011.

[6] H. Felice et al., “Design of HQ – a High Field Large Bore Nb_3Sn Quadrupole Magnet for LARP”, *IEEE Transactions on Applied Suprecond*., vol. 19, no. 3, part 2, pp. 1235-1239, 2009.

[7] S. Caspi et al., “Test Results of 15 T Nb_3Sn Quadrupole Magnet HQ01 with a 120 mm Bore for the LHC Luminosity Upgrade”, *IEEE Trans. on Applied Supercond*., vol. 21, No. 3, pp. 1854-1857, June 2011.

[8] A. Godeke et al., “A General Scaling Relation for the Critical Current Density of Nb_3Sn”, *Supercond. Sci. Technol.* 10 R100-R116, 2006.

[9] H. Felice et al., “Impact of Coil Compaction on Nb_3Sn LARP HQ Magnet”, *this conference*.

[10] M.J. Lamm et al., “A New Facility to Test Superconducting Accelerator Magnets” *Proceedings of PAC97*, pp. 3395-3397

[11] A.V. Zlobin *et al*., “R&D of Nb_3Sn Accelerator Magnets at Fermilab”, *IEEE Trans. Appl. Supercond.*, Vol. 15, 2005, p. 1113.

[12] D.F. Orris et al., "Voltage Spike Detection in High Field Superconducting Accelerator Magnets", *IEEE Trans. Applied Superconduct*., vol.15, no.2, pp. 1205-1208, June 2005.

[13] T. Salmi et al., “Quench Protection Challenges in Long Nb_3Sn Accelerator Magnets”, *presented at CEC/ICMC, 2011*.

[14] M. Marchevsky et al., “Test Results of HQ01, a 120 mm Bore LARP Quadrupole Magnet for the LHC Upgrade”, *this conference*.

[15] G. Chlachidze et al., “HQM01 magnet test summary”, Fermilab Technical Division Note TD-11-016.